Available online at www.sciencedirect.com
SCIENCE DIRECT®
Polymer 44 (2003) 8167–8176
polymer
www.elsevier.com/locate/polymer

Crystallization and orientation behaviors of poly(vinylidene fluoride) in the oriented blend with nylon 11

Yongjin Li, Akira Kaito*

Research Center of Macromolecular Technology, National Institute of Advanced Industrial Science and Technology (AIST), AIST Tokyo Waterfront, 2-41-6 Aomi, Koutou-Ku, Tokyo 135-0064, Japan

Received 12 March 2003; received in revised form 22 July 2003; accepted 8 October 2003

Abstract

Oriented films of nylon 11/poly(vinylidene fluoride) (PVDF) blend were prepared by uniaxially stretching the melt-mixed blends. The drawn films of fixed length were heat-treated at 170 °C for 5 min to melt the PVDF component, followed by quenching in ice water or isothermal crystallization at various temperatures. The crystal forms and orientation textures of the obtained samples were studied using wide-angle X-ray diffraction (WAXD) and small-angle X-ray scattering (SAXS). It was found that PVDF can crystallize into both α and β forms in the nylon 11/PVDF blends, and that the content of the β form increases with increasing crystallization temperature above 120 °C. The orientation behavior of the α-form PVDF was observed to be dependent on the crystallization conditions: *c*-axis orientation to the stretching direction was produced for the sample crystallized below 50 °C; the *a*-axis of α crystals was tilted from the stretching direction when PVDF was crystallized at about 75 °C; the parallel orientation of the *a*-axis to the stretching direction becomes dominant at higher crystallization temperatures (above 100 °C). In contrast, the β crystalline form maintains the *c*-axis orientation irrespective of crystallization temperature. It was shown by the confocal laser scanning microscopy that cylindrical domains of PVDF were dispersed in the oriented matrix of nylon 11. The mechanism for the formation of the unique orientation textures is discussed in detail. It was proposed that the *a*-axis orientation is a result of the *trans*-crystallization of PVDF in the cylindrical domains confined by the oriented matrix of nylon 11. The crystallization kinetics, WAXD analysis, and morphology studies preferred the *trans*-crystallization mechanism. The mechanical properties of the as-drawn and heat-treated samples were measured not only in the stretching direction but also in the direction perpendicular to it. It was found that the heat-treated samples show slightly lower tensile strength, but more elongation at the break in the two directions than the as-drawn samples.

Keywords: Polymer blend; Orientation; Crystallization

1. Introduction

Over the past several decades, a considerable amount of research has been performed in the field of polymer blends because it is expected that they will show some new and desirable properties [1]. Many researchers have extensively investigated the polymer blends including the mechanical properties, phase diagrams and morphological features. The orientation of polymer chains is also one of the important factors in controlling the properties of polymers. Therefore, there are some reports about the orientation behaviors of the amorphous/amorphous polymer blends [2–6]. All of these works are concerned with the different orientation behaviors of the two components during uniaxial stretching and the interactions between the two components in the blends [2–6].

Recently, several studies have been reported on the oriented crystallization of polymer blends containing crystalline polymer [7–9], which is also an attractive subject because it may lead to the formation of new superstructures for the blend systems. Prud'homme et al. have studied the crystallization and orientation behavior of poly(ϵ-caprolactone) (PCL) in the PCL/poly(vinyl chloride) (PVC) system [7] and the PCL/poly(styrene-co-maleic anhydride) (SMA) system [8]. They prepared the oriented blends of PCL with the amorphous polymers and then cold-crystallized them under strain. It was found for the PCL/PVC system that under most conditions, the crystallization under strain leads to a segmental crystalline orientation

* Corresponding author. Tel.: +81-3-3599-8307; fax: +81-3-3599-8166.
E-mail address: a-kaito@aist.go.jp (A. Kaito).

0032-3861/$ - see front matter © 2003 Elsevier Ltd. All rights reserved.
doi:10.1016/j.polymer.2003.10.014

perpendicular to the strain direction, whereas a parallel crystalline orientation can also be observed under conditions when the crystallization is more rapid and the draw ratio is higher. However, the molecular chains of the PCL in the PCL/SMA system is always oriented parallel to the strain direction. More recently the oriented crystallization has been examined for the isotactic polystyrene (iPS)/poly(phenylene oxide) (PPO) blend in our laboratory [9]. The *c*-axis of iPS crystals was found to be parallel to the stretching direction, but the orientation of the amorphous chains of PPO is relaxed. The mechanical properties for the iPS/PPO blend are improved as compared with those obtained for oriented pure iPS.

On the other hand, the studies on the orientation and crystallization behaviors have been extended to the immiscible blends of two crystalline polymers [10–16], such as melt-extruded biconstituent fibers [10,11], and a polypropylene (PP)/polyethylene (PE) system [14–16], where some unusual orientation textures of dispersed phase have been observed. The unique orientation behaviors have been explained either by epitaxial crystal growth on the polymer crystal [10–12] or by the thermal shrinkage stress [16]. The compatibility between the two components in the blend should have important effects on the orientation behaviors for the oriented blend systems consisting of two crystalline polymers. From this point of view, poly(vinylidene fluoride) (PVDF)/nylon 11 blend is an interesting system for the studies of oriented crystallization. Although PVDF/nylon 11 is not a miscible blend, the specific intermolecular interactions between the two semicrystalline polymers have been evidenced by the decrease of glass transition temperature and melting temperature of nylon 11 with increasing PVDF percent [17,18]. The crystallization-temperature-dependent orientation behavior of PVDF crystals in this crystalline/crystalline polymer blend has been reported elsewhere [19]. In this work, the mechanism of the unique oriented textures adopted by PVDF is investigated systematically. In addition, the mechanical properties of the oriented PVDF/nylon 11 blends were also studied.

2. Experimental section

2.1. Materials and sample preparation

PVDF and nylon 11 samples used in this study were purchased from Scientific Polymer Products and Aldrich Chemical Company, respectively. The two polymers at a weight ratio of 50/50 were melt-blended using a single-screw extruder. The temperatures of the three zones (feed zone, extruder zone and die) for the extruder were set to be 165, 185 and 210 °C, respectively. The blends were then hot pressed at 215 °C to a thin sheet with the thickness of 200 μm, followed by rapid quenching in ice water. Oriented samples (designated to be *as-drawn samples*) were prepared by uniaxially stretching the molded sheets to a draw ratio of 4 at 145 °C at a stretching speed of 10 mm/min. The as-drawn samples were heat-treated with fixed ends at 170 °C for 5 min to melt the PVDF component and then annealed at 120 °C for 3 h (designated to be *annealed-samples*) or quenched in ice water (designated to be *quenched samples*) to recrystallize PVDF.

2.2. Characterization

Differential scanning calorimetry (DSC) was measured under nitrogen flow at a heating rate of 10 K/min with a Perkin Elmer DSC-7 differential scanning calorimeter calibrated with the melting temperatures of indium and zinc. The crystallization kinetics studies were also carried out with the differential scanning calorimeter. The samples were first heated to 175 °C, kept at this temperature for 15 min and then cooled (200 °C/min) to 140 °C for isothermal crystallization.

Wide-angle X-ray diffraction (WAXD) diagrams were measured using a Cu Kα radiation (40 kV, 300 mA) generated by an X-ray diffractometer, Rigaku, Rint 2500 VH/PC and an image plate as the detector. The WAXD profiles with the reflection and transmission modes were obtained by a scintillation counter and a goniometer. The degree of orientation of the crystal axes was determined from the azimuthal intensity distribution of the corresponding reflections, which were obtained by rotating the sample at a fixed angle of 2θ. Small-angle X-ray scattering (SAXS) patterns were obtained by a fine-focused Cu Kα radiation (45 kV, 60 mA) generated by an X-ray diffractometer, Rigaku, Ultrax 4153A 172B and by an imaging plate detector. Polarized FTIR spectra were measured with a Digilab FTS 6000ec spectrophotometer and a wire-grid polarizer.

A scanning electronic microscope (SEM), Philips, XL30 ESEM FEG was used to observe the fracture surface morphology of the blends. The samples were fractured in liquid nitrogen and the surface was coated with a thin layer of gold. Confocal laser scanning microscope (CLSM) measurements were carried out with a laser-scanning microscope, Zeiss LSM 510. The blend was dyed with the fluorescent dye, fluorescein (Wako Pure Chemical Industries, Ltd) prior to the observation. It was found that only nylon 11 can be stained, but PVDF cannot be stained with the fluorescent dye in the blend.

Mechanical properties were measured both in the stretching direction and in the direction perpendicular to it. Rectangle-shaped specimens with 2 mm width and 20 mm length were cut from the sample in the two directions, and were used for the tensile test. Tensile tests were carried out at a rate of 2 mm/min at 20 °C and 50% relative humidity, using a tensile testing machine, Tensilon UMT-300 (Orientec Co. Ltd).

3. Results and discussion

3.1. Thermal properties

Fig. 1 shows the DSC curves of PVDF, nylon 11 and PVDF/nylon 11 blends during the melting and crystallization processes. Two specific melting and crystallization peaks can be observed for the blend system, which means that PVDF and nylon 11 melt and crystallize separately in the blends. Crystalline melting temperature of Nylon changes from 193 to 189 °C after blending, but that of PVDF is not much changed. The decrease of melting temperature of nylon 11 in the blends indicates that there are some interactions between the two polymers, which is consistent with the results of Gao et al. [17,18]. It is also found from Fig. 1 that PVDF is completely melted at 170 °C, but nylon 11 crystals are preserved at this temperature. Therefore, 170 °C was selected to be the heat-treatment temperature to melt PVDF in the following experiments.

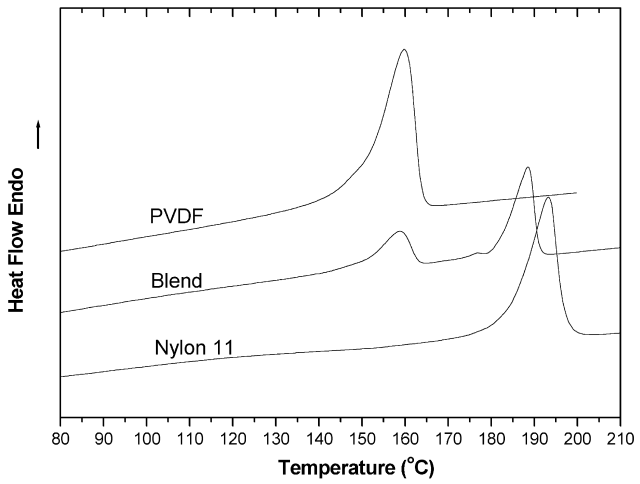

(a)

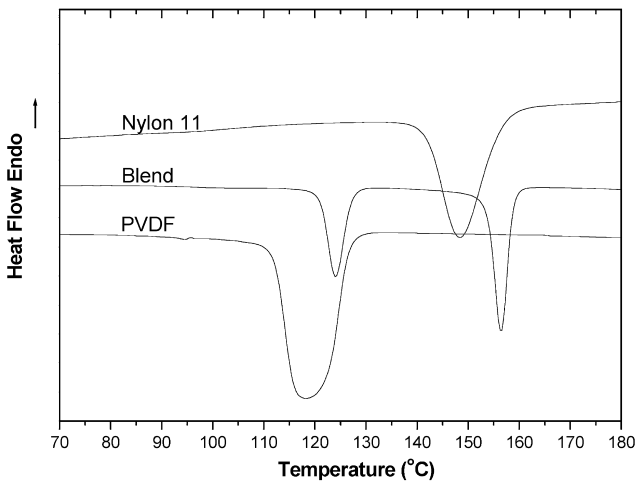

(b)

Fig. 1. DSC curves of PVDF, PVDF/nylon 11 blend, and nylon 11: (a) melting endotherms, and (b) crystallization exotherms.

3.2. Orientation behaviors

It is well known that PVDF can crystallize into at least five different crystal forms [20,21]. The α form is the most common crystal phase and it can be obtained by the conventional melt-crystallization method. The β-form has a planar (all *trans*) zigzag conformation and only the β-form shows ferroelectric properties. The α-form can be transformed into the β-form by stretching at room temperature.

The WAXD diffraction patterns for the as-drawn, quenched and annealed samples are shown in Fig. 2. The (*hk*0) reflections of both nylon 11 and PVDF are observed only on the equator for the as-drawn blends, which reveals the superposition of the *c*-axis orientation textures of the two polymers (Fig. 2(a)). The quenched sample shows the same diffraction pattern as that of the as-drawn sample and adopts the *c*-axis orientation textures (Fig. 2(b)). However, a totally different orientation texture can be observed for the annealed samples as shown in Fig. 2(c). The (100) reflection of the α form of PVDF was found to move to the meridian while the (020) reflection is still located on the equator, which means that the *a*-axis becomes parallel to the stretching direction. It is difficult to discern the orientation behavior of the β-crystals from the equatorial reflections because the equatorial reflections of the α form are much overlapped with the reflections of nylon 11. However, the characteristic (001) reflection of the β form can be observed if we tilt the sample by 15° from the vertical direction during the WAXD measurements (Fig. 2(d)). Thus, the β form coexists with the α form for the sample crystallized in the blends with nylon 11.

Fig. 3 shows the meridional WAXD profiles for the quenched sample and samples annealed at different temperatures. Both the characteristic (002) reflection for the α-form and the (001) reflection for the β-form can be observed for all samples, which indicates that PVDF crystallized into both α and β forms for the quenched and annealed samples. The WAXD profiles are affected not only by the crystal orientation but also by the relative amounts of the α and β forms. The intensity of the (002) reflection of the α form decreases and that of the (100) reflection increases with increasing annealing temperature from 50 to 85 °C; these changes can be attributed to the orientation change of the α crystalline form from the *c*-axis orientation to the *a*-axis orientation. On the other hand, the intensity of the (002) reflection of the α form decreases and the (001) reflection of the β form is intensified with the rise in annealing temperature from 120 to 130 °C. The amount of the β form increases with increasing annealing temperature in this temperature range. The result is rational because it has been reported that PVDF easily crystallizes into the β-form when crystallized at high temperatures [22].

The orientation functions for crystal axes of the α and β

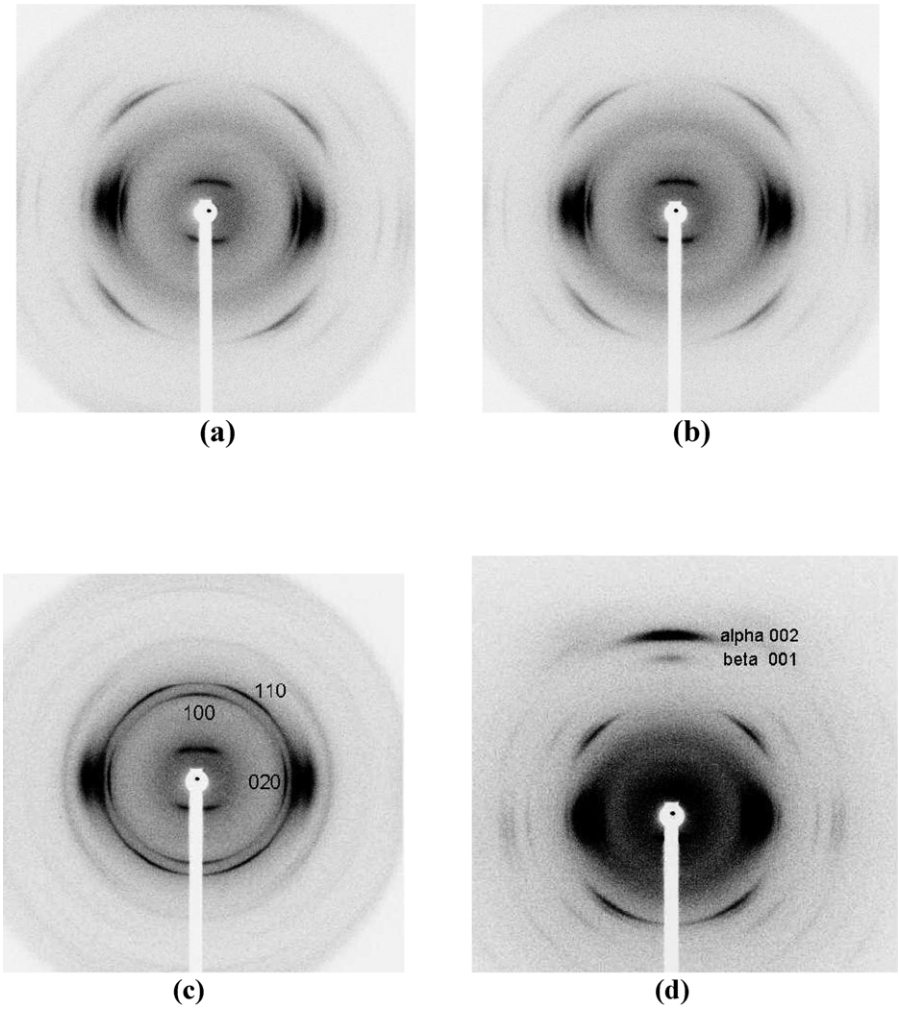

Fig. 2. WAXD patterns of PVDF/nylon 11 blends: (a) as-drawn sample, (b) quenched sample, (c) annealed sample, and (d) tilt measurements for the quenched sample.

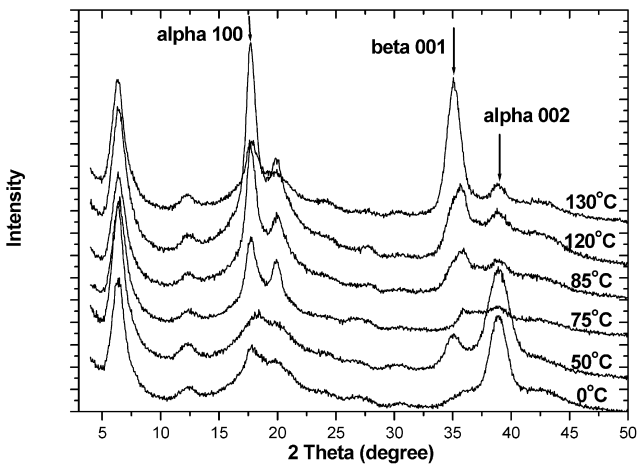

Fig. 3. Meridional WAXD profiles for the samples crystallized at indicated temperatures.

forms are obtained from the azimuthal intensity distribution of crystalline reflections. The WAXD intensity distribution, $I(\theta, \varphi)$ is expressed as functions of Bragg angle, θ, and the azimuthal angle, φ. The subtraction of background intensity was carried out as follows:

$$I(\varphi)_c = I(\theta_p, \varphi) - I(\theta_{b1}, \varphi) \times C_1 - I(\theta_{b2}, \varphi) \times C_2 \quad (1)$$

$$C_1 = \theta_{b2}/(\theta_{b1} + \theta_{b2}) \quad (2)$$

$$C_2 = \theta_{b1}/(\theta_{b1} + \theta_{b2}) \quad (3)$$

$I(\theta_p, \varphi)$ is the azimuthal intensity distribution of the crystalline reflection of interest, whose peak is observed at θ_p, and $I(\theta_{b1}, \varphi)$ and $I(\theta_{b2}, \varphi)$ are the intensity distributions of backgrounds at θ_{b1} and θ_{b2} ($\theta_{b1} < \theta_p < \theta_{b2}$). The orientation functions are calculated from the corrected WAXD intensity distribution.

$$\langle \cos^2 \varphi \rangle = \int_0^{\pi} I(\varphi)_c \cos^2 \varphi \sin \varphi \, d\varphi \Big/ \int_0^{\pi} I(\varphi)_c \sin \varphi \, d\varphi \quad (4)$$

$$f = (3\langle \cos^2 \varphi \rangle - 1)/2 \quad (5)$$

The orientation functions of the crystal a- and b-axes, f_a and

f_b, for the α form were obtained from the intensity distribution of the (100) and (020) reflections, respectively. The orientation function of the *c*-axis, f_c, was obtained from the relationship that holds for the orientation functions of pseudo-orthorhombic crystal lattice.

$$f_a + f_c + f_c = 0.0 \quad (6)$$

On the other hand, the equatorial reflections of the β forms markedly overlap with the reflections of nylon 11. The orientation function of the *c*-axis of the β form was obtained directly from the azimuthal intensity distribution of the (001) reflection of the β form.

Fig. 4 shows the azimuthal profiles of (100) reflection of the α form after subtracting the background. For the sample that crystallized at 50 °C, the reflection peaks locate at $\varphi = \pm 90°$, indicating the presence of *c*-axis oriented textures. However, two strong peaks at $\varphi = \pm 58°$ can be observed when crystallized at 75 °C, which means that the *a*-axis is tilted by 58° from the stretching direction for this sample. In addition, a small peak appeared at 0° indicating that there is a small amount of α crystals with *a*-axis orientation. With increasing crystallization temperature, the intensity of the two peaks at $\varphi = \pm 58°$ decreases and the intensity of the peak at $\varphi = 0°$ increases gradually. The change of the azimuthal profile with crystallization temperature shows that the amount of tilted orientation of the *a*-axis decreases and that of parallel orientation increases with increasing crystallization temperature. Finally, the crystals with the *a*-axis orientation become dominant when the samples are crystallized at higher temperatures (above 100 °C).

The crystal orientation functions for the α and β forms are summarized as a function of annealing temperature in Fig. 5. The orientation function of the *a*-axis of the α crystalline form increases from a negative value to a positive value with increasing crystallization temperature in the temperature range of 50–85 °C. Accordingly the orientation function of the *c*-axis of the α crystal decreases with increasing crystallization temperature in the same temperature range. For the samples crystallized above 85 °C, the crystal *a*- and *b*-axes are oriented parallel and perpendicular, respectively, to the drawing direction, and the orientation functions of the *c*-axis are in the range of $f = -0.1$ to 0.25. On the other hand, the value of orientation function for the *c*-axis of the β form is as high as 0.95–0.98 in the crystallization temperature range of 0–130 °C, indicating that the β crystalline form maintains a high degree of *c*-axis orientation irrespective of crystallization temperature.

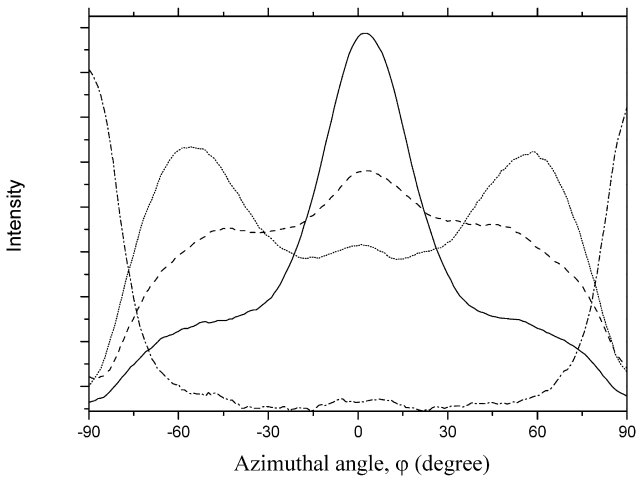

Fig. 4. Azimuthal profile of (100) reflection of the α-form crystal crystallized at the indicated temperatures after subtracting the background (0° and ±90° corresponds to the meridian and the equator direction, respectively): (—) 130 °C, (– – –) 100 °C, (· · ·) 75 °C, and (·–·–·–) 50 °C.

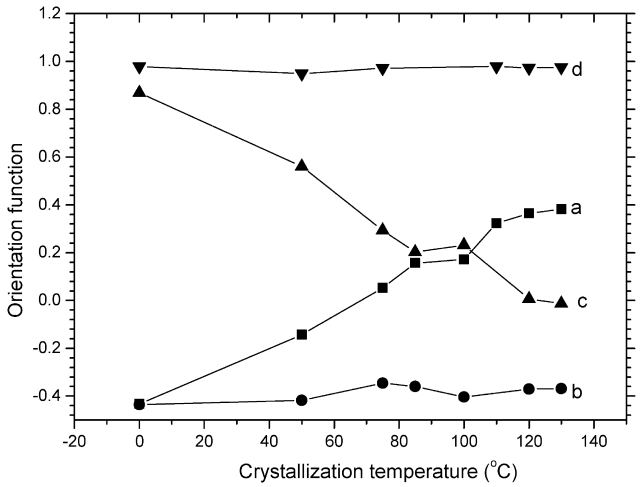

Fig. 5. Relationship between the crystalline orientation functions and the crystallization temperature for the α and β crystals: (a) f_a of the α-form, (b) f_b of the α-form, (c) f_c of the α-form, and (d) f_c of the β-form.

3.3. Morphologies

The fracture surface morphology, which was observed by SEM, is shown in Fig. 6(a). The rod-like units with a diameter of about 3 μm are oriented to the drawing direction. The coarse surface morphology suggests that the sample was fractured at the interface of the domains of the two polymers. Fig. 6(b) shows the internal morphology observed by CLSM. It is evident from the CLSM image that the PVDF/nylon 11 blend is not a miscible blend system. PVDF forms cylindrical domains with a diameter of about 2–5 μm and a length of about 30 μm, which are dispersed in the matrix of nylon 11. The nylon 11 matrix will surround the PVDF melts when the blend is heated to a temperature between the melting temperatures of the two components. It is possible that the interface of nylon 11 and PVDF can act as the nucleation site during the crystallization of PVDF, which is confirmed by the crystallization kinetics of PVDF in the blend.

Fig. 7 shows the SAXS patterns of the as-drawn and heat-treated samples measured both at room temperature and at 170 °C. The scattering lobes are only located in the vertical direction for the as-drawn and quenched samples indicating

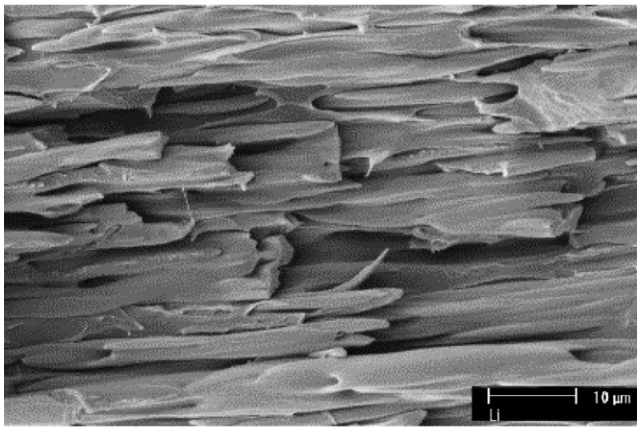

(a)

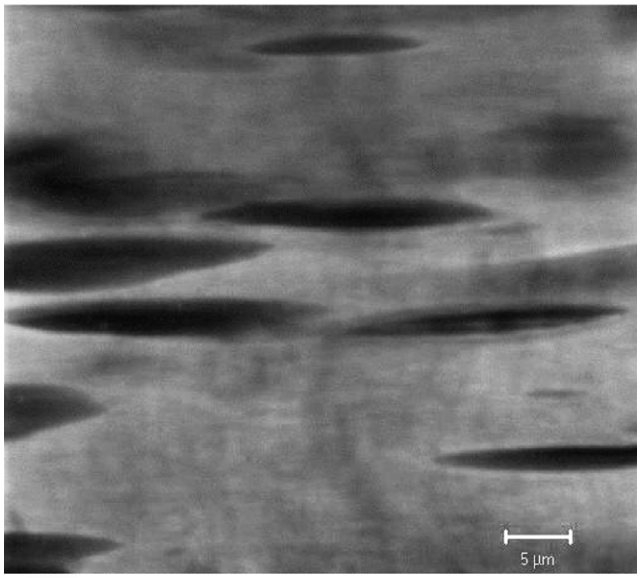

(b)

Fig. 6. Morphologies of the as-drawn PVDF/nylon 11 blend: (a) SEM image, and (b) CLSM image (drawing direction is horizontal).

that the lamellar stacks of both PVDF and nylon are oriented along the stretching direction. For the annealed sample, however, arc-like scattering is observed in the whole directions. The scattering is considered to originate only from the lamellar stacks of PVDF, because it disappears completely above the melting temperature of PVDF (Fig. 7(d)). The lamellar stacks of PVDF are distributed in various directions inside the cylindrical domains of PVDF. The SAXS results show that the supermolecular structure of the annealed sample changes during the isothermal crystallization at 120 °C, which is consistent with the WAXD results.

3.4. Mechanical properties

The mechanical properties of the as-drawn, quenched and annealed samples are characterized both in the stretching direction and in the direction perpendicular to it. The results of the stress–strain curves of the three samples are shown in Fig. 8. The samples after heat-treatment show more elongation at the break in both of the two directions than the samples before annealing. It is commonly accepted that the ductility (elongation) of polymer materials is mainly determined by the amorphous part in semicrystalline polymers [23]. Not only the crystals but also the molecular chains in the amorphous phase are oriented to the drawing direction for the as-drawn samples. The heat-treatment at 170 °C makes the oriented chains in the amorphous phase partially relaxed. Therefore, the heat-treated samples show more elongation at the break than the as-drawn sample. Annealing the sample at 120 °C for a long time also leads to the relaxation of amorphous chains and hence to the greatest elongation at the break in the two directions.

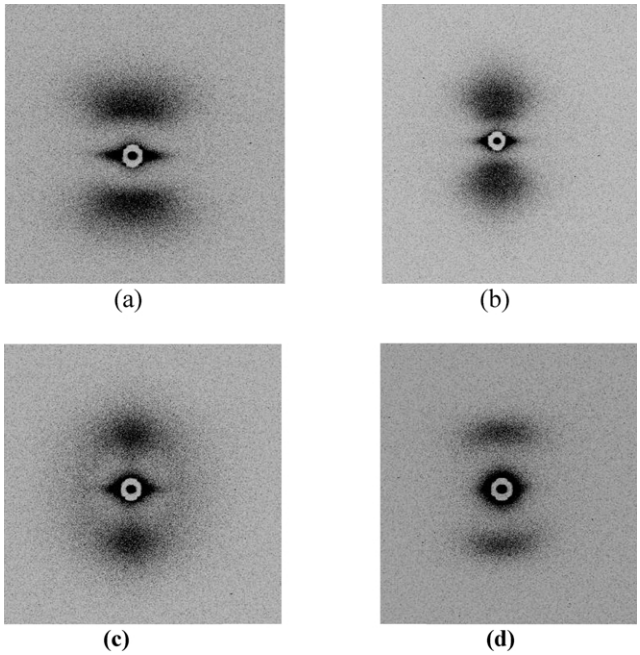

(a) (b) (c) (d)

Fig. 7. SAXS patterns of PVDF/nylon 11 blends: (a) as-drawn sample measured at room temperature, (b) quenched sample measured at room temperature, (c) annealed sample measured at room temperature, and (d) annealed sample measured at 170 °C.

3.5. Crystallization kinetics

The experiments of crystallization kinetics of pure PVDF and PVDF in blends were carried out with the same procedure. The well-known Avrami equation [24] was used to determine the characteristic parameters of polymer nucleation and crystal growth, as follows:

$$\mathrm{Log}\{-\ln(1-X_t)\} = n\log t + \log K$$

where t is the crystallization time, X_t is the relative degree of crystallinity at t, and n is the Avrami exponent dependent on the nucleation and growth geometry of the crystals. The plots of $\log(-\ln(1-X_t))$ against $\log t$ for the pure isotropic

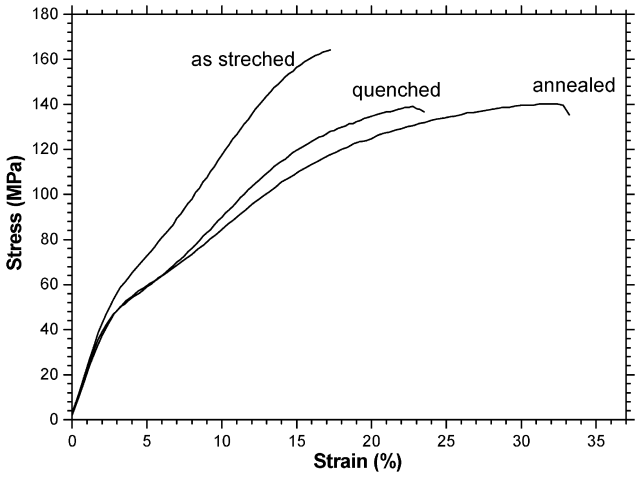

(a)

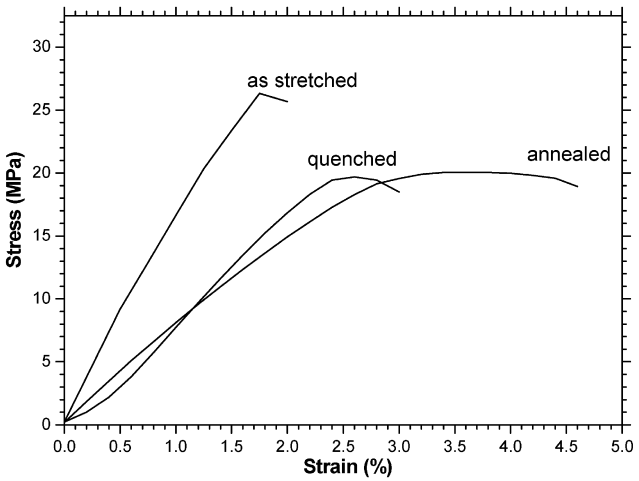

(b)

Fig. 8. Stress–strain curves of the oriented blends: (a) parallel direction, and (b) perpendicular direction.

PVDF, isotropic blend, and oriented blend are shown in Fig. 9. The Avrami exponent n can be determined as the slope of the curve by a linear regression. The decrease of n from 2.9 for pure PVDF to 2.0 for the blends indicates that the nucleation mechanisms are different. The decrease in the exponent for the blend sample is possibly attributed to the heterogeneous nucleation of PVDF on the surface of the nylon11 matrix. It seems that the orientation of the matrix influences not only the nucleation but also the growth of PVDF crystals because the Avrami exponent is only 1.5 for the oriented blend.

3.6. Crystallization of thin film of PVDF sandwiched by nylon films

It can be concluded from the above experiments that PVDF crystallizes in the cylindrical domains confined by

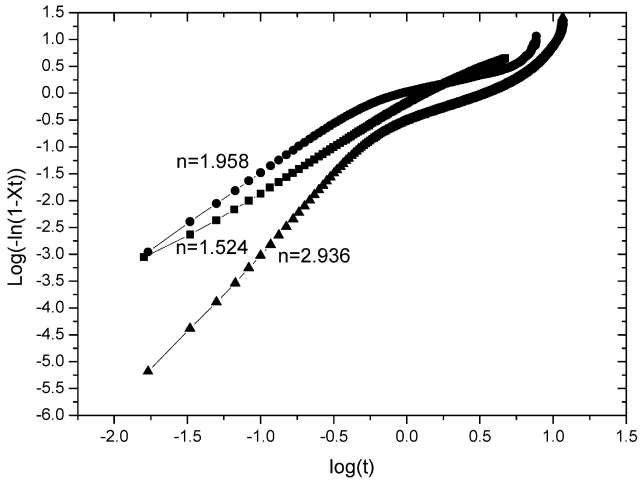

Fig. 9. Avrami plots of PVDF crystallized from pure PVDF (▲), isotropic PVDF/nylon 11 blend (●), and oriented PVDF/nylon 11 blend (■).

the oriented matrix of nylon 11 (from SEM and CLSM images) and that the matrix acts as heterogeneous nuclei for the crystallization of PVDF (from the crystallization kinetics studies). In order to discuss the mechanism for the oriented crystallization, another experiment was carried out. We have analyzed the oriented structures in a PVDF film that crystallized between the oriented nylon 11 films and compared the orientation in the PVDF film with those in the PVDF/nylon 11 blends. A PVDF film (about 70 μm in thickness) was sandwiched between two oriented nylon 11 films and heat-treated at 170 °C for 5 min and then cooled to 120 °C for isothermal crystallization for 3 h. The obtained PVDF film was examined by WAXD with the transmission and reflection modes as shown in Fig. 10. The scattering vector is normal to the film plane in the case of reflection mode, but it is parallel to the film plane for the transmission mode. It is evident that the diffraction intensity of the (020) reflection relative to the intensities of other reflections is higher for the reflection mode than for the transmission

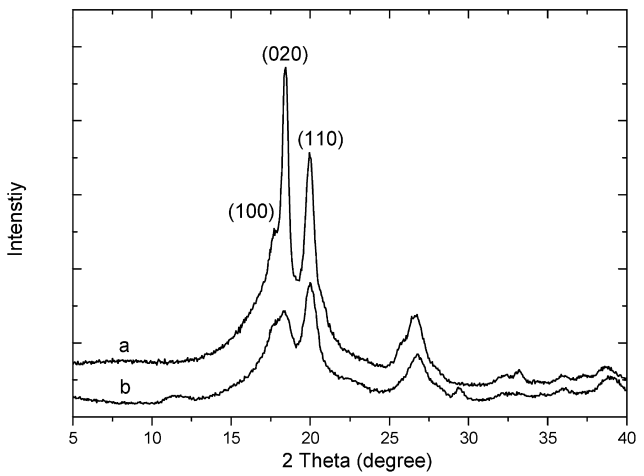

Fig. 10. WAXD diagrams for a PVDF film crystallized between oriented nylon films at 120 °C for 3 h: (a) reflection measurement, and (b) transmission measurement.

mode, which means that the *b*-axis of the α-form is oriented perpendicular to the film plane. Stein et al. [25] have also reported that the crystal *b*-axis of the α form is oriented to the direction of crystal growth when crystallized from the melt and that the *b*-axis is the axis of crystal growth. This means that the crystal growth proceeds normal to the film plane when the PVDF is crystallized between two nylon films (as shown in Fig. 11(a)). The crystallization of PVDF in the oriented blend with nylon 11 can be explained in the analogous way (Fig. 11(b)); the crystal of PVDF grows along the direction normal to the axis of the cylindrical domains in the blend with nylon 11.

A thin PVDF film of 15 μm thickness was sandwiched between two oriented nylon films and crystallized from the melt at various temperatures. Fig. 12 shows the polarized FTIR spectra of the PVDF film crystallized between oriented nylon films. The transition moment directions for the 1056, 612, 489 cm^{-1} bands are parallel to the molecular chain axis, whereas those for the 976, 853, 766, 532 cm^{-1} bands are perpendicular to the chain axis [26]. The polarized FTIR spectrum reveals that molecular chains of the α form are oriented parallel to the orientation direction of nylon 11. Thus the parallel alignment of molecular chains of PVDF along the orientation direction of nylon is induced by crystallization of PVDF on the oriented nylon films, due to the specific interaction of the two polymers at the interface. The degree of orientation is lower for the sample crystallized at 120 °C than for the sample quenched in ice water.

The weak absorption bands with perpendicular polarization were observed at 508 and 840 cm^{-1}, and these absorption bands can be assigned to the A_1 and B_2 vibrations, respectively, of the β crystalline form [27]. It was shown that a small amount of the β form was induced in the film crystallized between oriented nylon films, and that

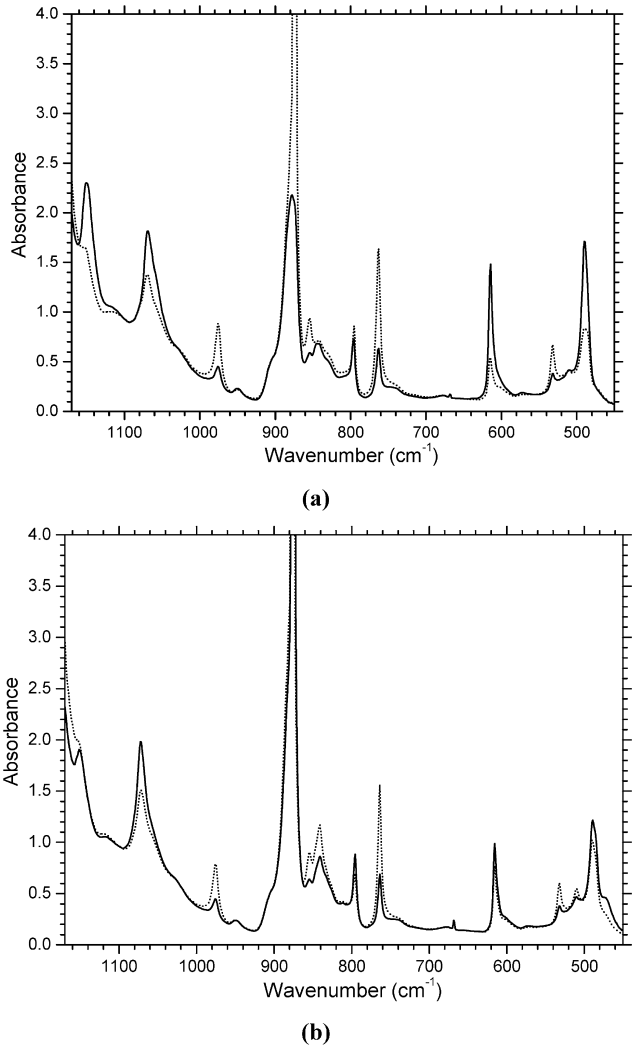

Fig. 12. Polarized FTIR spectra of PVDF films crystallized between oriented nylon films (—) parallel direction, (···) perpendicular direction: (a) quenched in ice water, and (b) crystallized at 120 °C for 3 h.

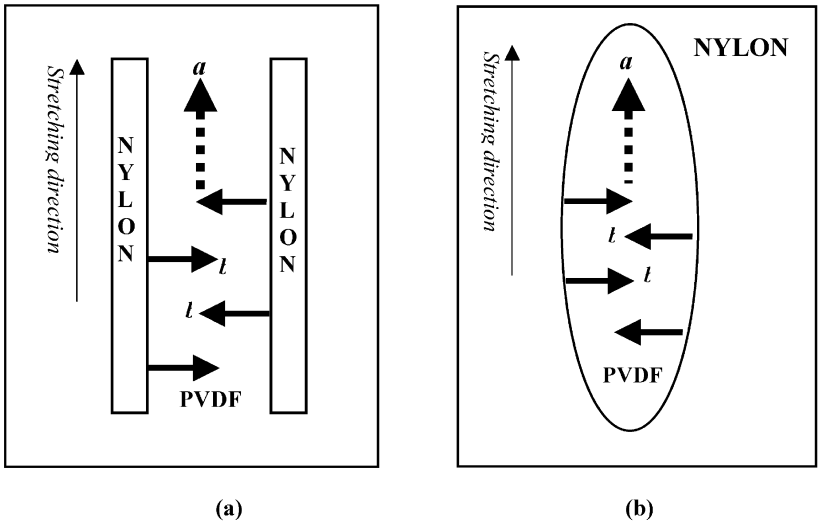

Fig. 11. Schematic representation of *trans*-crystallization of PVDF (a) in the film sandwiched between two oriented nylon 11 films; (b) in the domain confined by oriented nylon 11 matrix.

the molecular chains of the β form were also oriented parallel to the orientation direction of nylon 11. The intensity of the absorption bands of the β form is higher at higher crystallization temperatures, suggesting that the amount of the β form increases with increasing crystallization temperature.

3.7. Mechanism for the oriented crystallization of PVDF in the oriented blends with nylon 11

It is interesting to elucidate the mechanism of the unique orientation behavior. Up to now, epitaxial crystallization [10–12], thermal shrinkage stress [13] and confined-growth crystallization [28] have been used to interpret some new crystalline textures found in some biconstituent fibers and PP/PE blends. The possibility of an epitaxial crystallization of PVDF on the surface of nylon 11 can be ruled out because different orientation textures were produced under different crystallization conditions. We could not find any evidence of lattice matching between the crystals of PVDF and nylon 11.

When the sample is quenched to low temperature (< 50 °C), the nucleation occurs at the interface of PVDF/nylon 11 with the molecular chains of PVDF parallel to the orientation direction of nylon 11. The parallel orientation of molecular chains of PVDF at the interface of PVDF/nylon 11 was confirmed by the measurement of polarized FTIR spectra for the PVDF film crystallized between oriented nylon 11 films (Fig. 12). It is considered from this result that the *c*-axis orientation of the α form in the oriented blend with nylon 11 is induced by the specific interaction of the two polymers. On the other hand, the *a*-axis is found to orient parallel to the stretching direction when crystallization temperature is higher than 100 °C. The relaxation of the PVDF chains may occur during crystallization at high temperatures, which is considered to be responsible for the temperature-dependent orientation change. We consider that the unique orientation textures are a result of the *trans*-crystallization of PVDF on the nylon 11 matrix. In fact, Benkhati et al. [29] have reported that the *trans*-crystallization phenomenon of PVDF is induced by several polymeric substrates. In the case of PVDF/nylon 11 blends, it is considered that the nucleation occurs at the interface of the domains and the crystals grow in the direction perpendicular to the axis of the cylindrical domains (as shown in Fig. 11(b)). The *trans*-crystallization mechanism is also supported by the decrease of Avrami exponent for the crystallization of oriented PVDF/nylon11 blend with respect to the crystallization of pure PDVF. Thus the crystal *b*-axis is highly oriented normal to the drawing direction, and the *a*-axis was obliged to align to the drawing direction when crystallized above 100 °C.

It should be mentioned that the β-forms of PVDF have an all-*trans* zigzag conformation and the parallel orientation of the molecular chains of β-PVDF may be stabilized by the strong interaction between the amide group of nylon 11 and CF_2 group of PVDF [17,18]. Therefore, the *c*-axis orientation of the crystals is preserved irrespective of the crystallization conditions.

4. Conclusions

Oriented crystallization of PVDF in the oriented blend with nylon 11 was studied under various crystallization conditions. It was found that PVDF can crystallize into both α and β forms in the oriented blend with nylon 11, and that the content of the β form increases with increasing crystallization temperature above 120 °C. The crystal *c*-axis of the β crystalline form is highly oriented to the drawing direction irrespective of the crystallization conditions. This may be because the oriented structure of the β-form of PVDF is stabilized by the intermolecular interaction between PVDF and nylon 11. On the other hand, the orientation textures of the α crystalline form crystallized from the oriented blends with nylon 11 are dependent on the crystallization conditions. When the sample is crystallized below 50 °C, the *c*-axis of the α crystalline form is oriented parallel to the stretching direction. In contrast, the *a*-axis is found to orient parallel to the stretching direction when crystallized above 100 °C. The tilted orientation of the *a*-axis from the stretching direction was produced at the crystallization temperatures of 75–100 °C. It is considered that the *c*-axis orientation is induced by the molecular interaction of PVDF and nylon 11 at the interface, and that the *a*-axis orientation textures crystallized at high temperature are a result of the *trans*-crystallization of PVDF in the confined domains. The orientation change is considered to originate from the relaxation of molecules with increasing crystallization temperature. The influence of the unique orientation textures on the properties of the blend was also investigated. It was found that the heat-treated oriented blends show more elongation at the break but lower tensile strength as compared with the as-drawn sample.

Acknowledgements

Y. Li thanks the Japan Society for the Promotion of Science (JSPS) for providing the fellowship and grant-in-aid to do this research at the National Institute of Advanced Industrial Science and Technology (AIST). This study is carried out as ‘Nanostructure Polymer Project’ (partially) supported by NEDO (New Energy and Industrial Technology Development Organization) launched in 2001.

References

[1] Paul DR, Newman S. Polymer blends. New York: Academic Press; 1978.

[2] Bouton C, Arrondel V, Rey V, Sergot P, Manguin JL, Jasse B, et al. Polymer 1989;30:1414.
[3] Gallagher GA, Jakeways R, Ward IM. J Polym Sci, Polym Phys 1991; 29:1147.
[4] Li D, Brisson J. Macromolecules 1997;30:8425.
[5] Rinderknecht S, Brisson J. Macromolecules 1999;32:8509.
[6] Pellerin C, Prud'homme R, Pézolet M. Macromolecules 2000;33: 7009.
[7] Zhao Y, Keroack D, Prud'homme R. Macromolecules 1999;32:1218.
[8] Morin D, Zhao Y, Prud'homme R. J Appl Polym Sci 2001;81:1683.
[9] Dikshit A, Kaito A. IUPAC World Polymer Congress 2002.
[10] Fornes RE, Grady PL, Hersh SP, Bhat GR. J Polym Sci, Polym Phys 1976;14:559.
[11] Seth KK, Kempster CJE. J Polym Sci, Polym Symp 1977;58:297.
[12] Takahashi T, Inamura M, Tsujimoto I. Polym Lett 1970;8:651.
[13] Takahashi T, Nishio Y, Mizuno H. J Appl Polym Sci 1987;34:2757.
[14] Gross B, Peterman J. J Mater Sci 1984;19:105.
[15] Kojima M, Satake H. J Polym Sci, Polym Phys 1984;22:285.
[16] Nishio Y, Yamane T, Takahashi T. J Macromol Sci—Phys 1984;B23: 17.
[17] Gao Q, Scheinbeim JI, Newman BA. J Polym Sci, Polym Phys 1999; 32:3217.
[18] Gao Q, Scheinbeim JI. Macromolecules 2000;33:7564.
[19] Li YJ, Kaito A. Macromol Rapid Commun 2003;24:255.
[20] Weinhold S, Litt MH, Land JB. J Polym Sci, Polym Lett 1979;17:585.
[21] Richardson A, Hope PS, Ward IM. J Polym Sci, Polym Phys 1983;21: 2525.
[22] Spector KS, Stein RS. Macromolecules 1991;24:2083.
[23] He MJ, Chen XW, Dong XX. Polymer physics. Shanghai: Fudan University Press; 1991.
[24] Avarami M. J Chem Phys 1939;7:1103.
[25] Morra BS, Stein RS. Polym Engng Sci 1984;24:311.
[26] Cortili G, Zerbi G. Spectrochim Acta 1967;23A:285.
[27] Kobayashi M, Tashiro K, Tadokoro H. Macromolecules 1975;8:158.
[28] Mencik Z, Plummer HK, Van Oene H. J Polym Sci, Part A-2 1972;10: 507.
[29] Benkhati H, Tan TTM, Jungnickel B-J. J Polym Sci, Polym Phys 2001;39:2130.